Elastic constants of BCC binary alloys near the A_3B composition and their relation to martensitic transitions

1990 J. Phys.: Condens. Matter 2 1743

(http://iopscience.iop.org/0953-8984/2/7/006)

J. Phys.: Condens. Matter **2** (1990) 1743–1752. Printed in the UK

Elastic constants of BCC binary alloys near the A_3B composition and their relation to martensitic transitions

T Castán, E Vives and A Planes

Departament d'Estructura i Constituents de la Matèria, Facultat de Física, Universitat de Barcelona, Diagonal 647, 08028 Barcelona, Catalonia, Spain

Received 2 June 1989, in final form 19 September 1989

Abstract. The present work deals with the analysis of the atomic-order dependence of the elastic constants of a BCC binary alloy near the A_3B composition. We assume that each atom interacts with nearest and next-nearest neighbours through a pairwise interatomic potential. The configurational phase diagram of the system has been obtained from Monte Carlo simulation of a lattice model for such an alloy system. The DO_3, B2 and A2 phases are found to be stable for appropriate values of the interaction parameters.

The elastic constants of partially ordered configurations are calculated at $T = 0$ K, after quenches from different temperatures T_q ranging over the stability regions of the three phases. The results are compared with experimental data corresponding to the Cu–Zn–Al shape memory alloy and their relevance in connection with the martensitic transformation is discussed.

1. Introduction

Elastic constants of solids are intrinsically related to lattice stability. They depend on composition and temperature (Born and Huang 1956). In the case of metallic alloys undergoing an order–disorder transition, the elastic constants exhibit an additional dependence on the configurational ordering state which, in turn, depends on temperature. This extra contribution is revealed experimentally by an anomalous behaviour of the elastic constants around the order–disorder transition point (MacManus 1969).

Theoretical expressions of isothermal elastic constants involve ensemble averages of functions of particle coordinates and of interparticle potential energies (Squire *et al* 1969). Their calculation, which is believed to be a hard task, can be done by using Monte Carlo (Ray 1988, Castán *et al* 1989) or molecular dynamics (Ray 1988) techniques.

Here we deal with BCC alloy systems which exhibit, from low to high temperatures, DO_3, B2 and A2 ordered structures. Examples are the Fe_3Al, Cu_3Al and Fe_3Pt binary alloys, and the Cu–Zn–Al or the Cu–Ni–Al ternary alloys. Some of these alloys (Fe_3Pt (ordered), Cu–Zn–Al and Cu–Ni–Al) are found to be shape memory alloys (SMA). From a practical point of view, these materials are of great importance because of their very interesting thermomechanical properties (shape memory effect, pseudoelasticity, high damping capacity) which are intimately related to the martensitic phase transition (MPT) that they undergo at low temperatures (Delaey *et al* 1974). Such a transition is a displacive first-order transition from a BCC to a close-packed structure, mainly described by a shear deformation on the {110} planes along the $\langle 1\bar{1}0 \rangle$ directions. Close to the MPT point (M_s),

0953-8984/90/071743 + 10 $03.50

the shear elastic modulus $C' = \frac{1}{2}(C_{11} - C_{12})$ presents an 'abnormal' behaviour (Guénin and Gobin 1982): (i) its value is small (in relation to the other relevant elastic constants of a cubic lattice), and (ii) decreases with decreasing temperature. Zener (1947) first predicted that the large elastic anisotropy due to the small value of C' stabilises the β-phase at high temperature by a large vibrational entropy, but the stability against a $\{110\}\langle 1\bar{1}0\rangle$ shear is reduced at low temperature. This favours the MPT. The Zener picture has been recently confirmed from first-principles calculations for the (BCC) Zr system (Ye *et al* 1987) and in the case of Cu–Zn and Cu–Zn–Al alloys from the analysis of measurements giving the resolved shear stress to induce the transformation as a function of temperature (Romero and Ahlers 1989). In spite of these results, the experimental studies clearly show that these transitions are not soft-mode transitions. It has then been proposed (Lindgård and Mouritsen 1986) that the transition is rather a consequence of the anharmonic interaction between the homogeneous strain associated with C' and an inhomogeneous modulation. In the same framework, the martensitic transitions of Li (Gooding and Krumhansl 1988) and Ni_xAl_{1-x} (Gooding and Krumhansl 1989) have recently been studied with encouraging results.

The fact that C' depends on the atomic ordering state of the system makes this last quantity relevant in relation to the characterisation of the MPT. This idea is supported by both theory (Viñals *et al* 1984) and experiments (Rapacioli and Ahlers 1979) and gives rise to a dependence of M_s on the state of order of the system. In addition, it is known that the amount of order present in the system can be drastically changed by means of fast quenches (Planes *et al* 1981).

Very recently (Castán and Planes 1988), a Monte Carlo study of the relationship between C' and the state of order, described in terms of suitable order parameters, has been carried out for the (BCC) β-CuZn SMA. In order to eliminate the contribution arising from thermal effects, the equilibrium atomic-order configuration at a temperature T_q was suddenly quenched to $T = 0$ K. Then the elastic constants can be simply calculated in terms of the interaction potential energies.

In the present work we focus our attention on the BCC binary alloy A_xB_{1-x} close to the A_3B composition ($x \simeq 0.75$). We use an Ising-type model to describe the state of order of the system with interactions up to next-nearest neighbours. The calculation of the phase diagram allows the establishment of the stability range of the DO_3, B2 and A2 phases we are interested in. Following standard procedures, we assume pairwise additive potentials for nearest and next-nearest neighbours and analyse the dependence of the elastic constants on the configurational ordering state in the DO_3 and B2 regions. We find that the qualitative behaviour is independent of particular details of the potential. These results are discussed in relation to experimental data corresponding to the martensitic transformation of Cu–Zn–Al SMA.

2. Theoretical considerations

2.1. The model

In this section we briefly summarise the main features of the model used to describe the state of order of the BCC alloy A_xB_{1-x} when x is close to the stoichiometric composition ($x \simeq 0.75$).

Consider a binary alloy with the following configurational Hamiltonian:

$$H = \sum_{\mu=1}^{2} (N_{AA}^{(\mu)} \Phi_{AA}(r_\mu) + N_{BB}^{(\mu)} \Phi_{BB}(r_\mu) + N_{AB}^{(\mu)} \Phi_{AB}(r_\mu)). \tag{1}$$

$N_{\alpha\beta}^{(\mu)}$ (α, β = A, B) is the number of μ-neighbour $\alpha\beta$ pairs and $\Phi_{\alpha\beta}(r_\mu)$ its corresponding interaction potential energy when they are separated by a distance r_μ. We now introduce pseudo-spin variables (Gunton and Droz 1983) σ_i, which take the value 1 (-1) when the lattice site i is occupied by an atom A (B). Using spin language, the Hamiltonian (1) takes the form

$$H = J_1 \sum_{\langle ij \rangle_{NN}} \sigma_i \sigma_j + J_2 \sum_{\langle ij \rangle_{NNN}} \sigma_i \sigma_j + H_0(x). \tag{2}$$

The first sum refers to nearest neighbours (NN) and the second to next-nearest neighbour (NNN) pairs. J_1 and J_2 are the ordering energies for NN and NNN respectively, which have the form

$$J_k = \tfrac{1}{4}(\Phi_{AA}(r_k) + \Phi_{BB}(r_k) - 2\Phi_{AB}(r_k)) \qquad k = 1, 2. \tag{3}$$

x is the A-component atom fraction. Since N_A and N_B are respectively the numbers of atoms A and B, $x = N_A/N$, with $N = N_A + N_B$ being the total number of particles. The term $H_0(x)$ can be written as

$$H_0(x) = N[(2x - 1)h + h_0] \tag{4}$$

where

$$h = +2\,(\Phi_{AA}(r_1) - \Phi_{BB}(r_1)) + \tfrac{3}{2}(\Phi_{AA}(r_2) - \Phi_{BB}(r_2)) \tag{5a}$$

and h_0 is a constant given by

$$h_0 = (\Phi_{AA}(r_1) + \Phi_{BB}(r_1) + 2\Phi_{AB}(r_1)) + \tfrac{3}{4}(\Phi_{AA}(r_2) + \Phi_{BB}(r_2) + 2\Phi_{AB}(r_2)). \tag{5b}$$

Now we define the following dimensionless quantities:

$$E = (H - H_0(x))/J_1 = H/J_1 - (2x-1)Nh/J_1 - Nh_0/J_1 \tag{6}$$

$$W = J_2/J_1. \tag{7}$$

Finally we get

$$E = \sum_{\langle ij \rangle_{NN}} \sigma_i \sigma_j + W \sum_{\langle ij \rangle_{NNN}} \sigma_i \sigma_j. \tag{8}$$

2.2. Relation to the elastic constants

We introduce the effect of ordering by assuming that $N_{AB}^{(1)}$ and $N_{AB}^{(2)}$ are the mean values of these quantities in equilibrium at temperature T_q. The procedure simulates measurements of elastic constants after ideally fast quenches from T_q to temperatures T_f—low enough to neglect the role of thermal fluctuations. We have taken in all cases $T_f = 0$ K (Castán and Planes 1988).

Assuming pairwise additive central forces and interaction up to NNN, the elastic constants of a BCC binary crystal can be written, at $T = 0$ K, as (Castán and Planes 1988)

$$VC_{11} = A_{11} - \tfrac{1}{32}N_{AB}^{(1)}\tilde{\Phi}_J^{(1)} - \tfrac{1}{6}N_{AB}^{(2)}\tilde{\Phi}_J^{(2)} \tag{9a}$$

$$VC_{44} = VC_{12} = A - \tfrac{1}{32}N_{AB}^{(1)}\tilde{\Phi}_J^{(1)} \tag{9b}$$

$$VC' = A' - \tfrac{1}{12}N_{AB}^{(2)}\tilde{\Phi}_J^{(2)} \tag{9c}$$

where V is the volume of the system. The terms A_{11}, A and A' are given by the expressions

$$A_{11} = N_A(\tilde{\Phi}^{(1)}_{AA}/4 + \tilde{\Phi}^{(2)}_{AA}) + N_B(\tilde{\Phi}^{(1)}_{BB}/4 + \tilde{\Phi}^{(2)}_{BB}) \tag{10a}$$

$$A = (N_A\tilde{\Phi}^{(1)}_{AA} + N_B\tilde{\Phi}^{(1)}_{BB})/4 \tag{10b}$$

$$A' = (N_A\tilde{\Phi}^{(2)}_{AA} + N_B\tilde{\Phi}^{(2)})/2 \tag{10c}$$

and

$$\tilde{\Phi}^{(\mu)}_{\alpha\beta} = 4(\mathrm{d}^2\Phi_{\alpha\beta}(r)/\mathrm{d}(r^2)^2)_{r=r^0_\mu} \tag{11a}$$

$$\tilde{\Phi}^{(\mu)} = \tilde{\Phi}^{(\mu)}_{AA} + \tilde{\Phi}^{(\mu)}_{BB} - 2\tilde{\Phi}^{(\mu)}_{AB} \qquad \mu = 1, 2. \tag{11b}$$

In (11a), the derivatives are calculated at r^0_μ, which is the equilibrium distance between μ-neighbour pairs. A direct look at expression (9) shows that, in this approximation, C_{11} depends on both $N^{(1)}_{AB}$ and $N^{(2)}_{AB}$, whereas C_{44} and C' only depend on $N^{(1)}_{AB}$ and $N^{(2)}_{AB}$ respectively. We expect a NN and NNN approximation, which in turn ensures the mechanical stability of the BCC lattice (Milstein 1970) to be good enough to reveal the main effects associated with B2 and DO_3 orderings. Concerning the centrality of the potential, it is believed to be a poor approximation for BCC metal systems. In particular, Monte Carlo simulations of elastic constants at finite temperature (Castán *et al* 1989) show that a central potential cannot simultaneously reproduce the behaviour of all the elastic constants. Nevertheless, we expect this approximation to be good enough to analyse the effect of atomic ordering on the elastic constants after quenches to very low temperature. Also, eventual changes of the lattice parameter with atomic order should be considered. Available experimental data corresponding to the Cu_3Au (FCC) system indicate that changes of the lattice parameter with atomic order are very small (Roy *et al* 1974). Unfortunately, to our knowledge, no similar study has been done for the systems we are dealing with. However, experimental results show that the lattice parameter of β-CuZn presents only slight changes with composition (the lattice parameter changes by approximately 0.06% per 1% change in composition, Massalski and King 1961). Consequently the variation of the elastic constants with T_q are given by

$$V\,\delta C_{11}/\delta T_q = -\tfrac{1}{32}\tilde{\Phi}^{(1)}_f\,\delta N^{(1)}_{AB}/\delta T_q - \tfrac{1}{8}\tilde{\Phi}^{(2)}_f\,\delta N^{(2)}_{AB}/\delta T_q \tag{12a}$$

$$V\,\delta C_{44}/\delta T_q = -\tfrac{1}{32}\tilde{\Phi}^{(1)}_f\,\delta N^{(1)}_{AB}/\delta T_q \tag{12b}$$

$$V\,\delta C'/\delta T_q = -\tfrac{1}{12}\tilde{\Phi}^{(2)}_f\,\delta N^{(2)}_{AB}/\delta T_q. \tag{12c}$$

That is, with $\tilde{\Phi}^{(\mu)}_f(\mu = 1, 2)$ fixed, the behaviour of C_{11}, C_{44} and C' with T_q will be mainly controlled by the variation of $N^{(1)}_{AB}$ and $N^{(2)}_{AB}$ with T_q.

In alloy systems undergoing an MPT, it has been found that the MPT temperature changes after a quench from T_q. It has been justified that this change δM_s is, to a first approximation, proportional to the corresponding change in C' (Nakanishi *et al* 1968, Planes *et al* 1985)). That is,

$$\delta M_s = -K\delta C' \tag{13}$$

K is a positive constant related to the slope of the temperature variation of $C'(T)$ ($K^{-1} = \mathrm{d}C'/\mathrm{d}T$) close to but above M_s. For a given alloy, K is independent of temperature (Guénin *et al* 1977). If one additionally assumes K independent of the state of order, the results are consistent with experimental data (Castán and Planes 1989). Then,

$$\delta M_s/\delta T_q = -K\,\delta C'/\delta T_q. \tag{14}$$

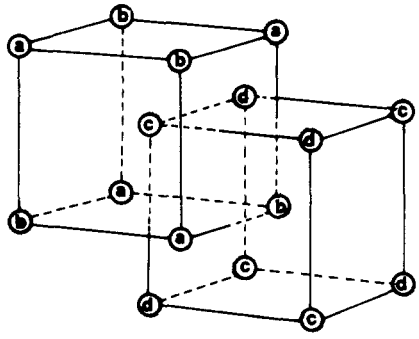

Figure 1. Sublattice structure of the BCC lattice

Let us specify that in the experimental procedure, the T_q-quenches are performed, to a final temperature T_f very close to but above M_s. Immediately afterwards, one continues decreasing the temperature and the MPT starts. Because of the diffusionless nature of the MPT, the state of order frozen at T_f will be preserved during the transformation. In addition, M_s is usually low enough to neglect thermal fluctuations. Hence, it can be assumed that the change in C' after the quench from T_q may be identified with the change obtained from equation (12). All these considerations enable us to write

$$\delta M_s/\delta T_q = (K\tilde{\Phi}_f^{(2)}/12\,V)\,\delta N_{AB}^{(2)}/\delta T_q. \tag{15}$$

This expression tells us that changes in M_s with T_q depend on the interaction potential through $\tilde{\Phi}_f^{(2)}$ and on the way $N_{AB}^{(2)}$ varies with the temperature T_q. Notice, however, that the role of the interaction potential is, in this approximation, limited to a coefficient in the linear relation between the T_q-variations of M_s and $N_{AB}^{(2)}$ and that (15) no longer implies any necessary reference to particular fine details of the interaction potential. The comparison between experimental M_s-behaviour and Monte Carlo calculations of $N_{AB}^{(2)}$, both as function of T_q, will give us information about the validity of these statements.

3. Results and discussion

In this section we present the Monte Carlo results corresponding to the equilibrium order behaviour of the alloy A_xB_{1-x} ($x \simeq 0.75$) described by the model (8), using appropriate interaction parameters. The ground state of the system has been analysed by Richards and Cahn (1971). A wide variety of phases can appear depending on the values of x and W. Particularly for $x = 0.75$ and $\frac{2}{3} > W > 0$, the ground state is DO_3, and for $x \neq 0.75$ but close to it, the ground state can show a mixture of the stoichiometric phases DO_3 and B2 or a gradual change in the occupancy of some of the sites due to the large degeneracy.

Calculations have been carried out following standard Monte Carlo techniques (Binder 1984). The system is a BCC lattice with $N = N_A + N_B = 2(8)^3$ particles obeying periodic boundary conditions. The volume of the system, $V = (8a)^3$, and the temperature remain fixed in each simulation. Starting from an initial random configuration, the system relaxes to the equilibrium state by means of a two-sites spin-exchange excitation mechanism.

In order to characterise the state of order of the system, let us define the following order parameters:

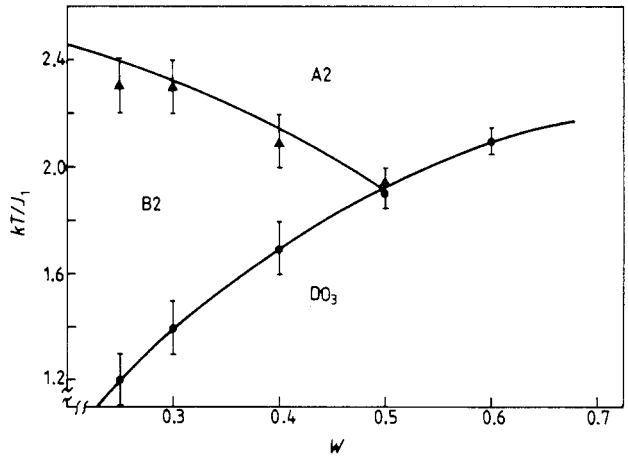

Figure 2. Phase diagram, for $x = 0.75$, showing the stability region of the A2, B2 and DO_3 phases obtained from Monte Carlo simulations.

$$m_\mu = 4\left(\sum_{i\in\mu}\sigma_i\right)\Big/N \tag{16}$$

where μ = (a, b, c, d) means the four equivalent sublattices usually defined to subdivide the BCC lattice (see figure 1).

In figure 2 we present the phase diagram for the stoichiometric composition ($x = 0.75$) within the range of interaction parameters $0 < W < \frac{2}{3}$. This is in agreement with previous Monte Carlo calculations (Dünweg and Binder 1987) and theoretical results (Bell 1987). One observes that when $W < 0.50$, the system passes through all three phases, DO_3, B2 and A2, when one moves along the temperature axis. For $W > 0.50$, the B2 phase does not appear and only the DO_3 and A2 phases are present.

To exemplify the procedure used to calculate the phase diagram, we show in figure 3 the behaviour of the order parameters (16) as a function of temperature for a value of the interaction parameter $W = 0.25$. In the same figure we have plotted both the Monte Carlo result and the mean-field calculation (Dünweg and Binder 1987). Near the transition points, finite-size effects cause the round shape exhibited by the order parameters, and introduce a quite important uncertainty in the determination of such points as T_{B2} and T_{DO_3}. We chose $W = 0.25$ to separate T_{B2} and T_{DO_3} in order to reveal the distinct effects of both transition points on the different properties of the system. In what follows we restrict ourselves to this value. Nevertheless, the same qualitative results are obtained with different values of W. In particular, we have also studied the cases $W = 0.20$, 0.30 and 0.40.

Figure 4 illustrates the temperature evolution of $N_{AB}^{(1)}$ and $N_{AB}^{(2)}$, when $x = 0.75$, calculated using Monte Carlo and mean-field techniques. One observes that both methods give the same qualitative behaviour for $N_{AB}^{(1)}$ and $N_{AB}^{(2)}$ across the range of temperatures. This is an unexpected result considering the disagreement between the values obtained from both techniques for the long-range order parameters (as displayed in figure 3). It means that mean-field calculations can provide quite good qualitative information about the variation of $N_{AB}^{(1)}$ and $N_{AB}^{(2)}$ with temperature. Consequently, this approximation, provided no more exact theories are available, is good enough to obtain qualitative information about the change of elastic constants with ordering.

In studying figure 4, one observes that $N_{AB}^{(1)}$ keeps nearly constant inside the DO_3 phase, whereas it shows a smooth decreasing in the B2 and A2 regions. Contrarily,

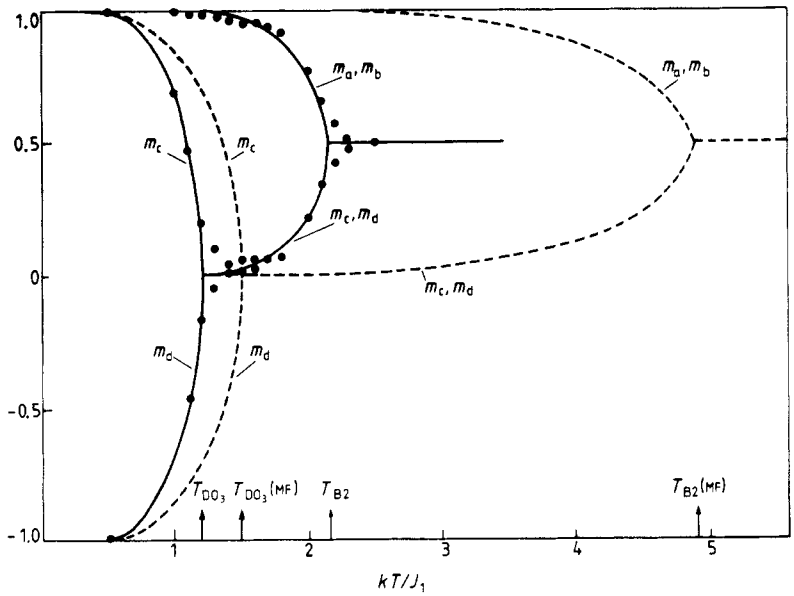

Figure 3. Long-range order parameters m_μ as a function of temperature for $x = 0.75$ and $W = 0.25$. The full circles correspond to Monte Carlo results and the full curves are just guides to the eye. Notice that near the transition temperatures, Monte Carlo results exhibit tails due to finite-size effects. The broken curves correspond to the mean-field solution. The arrows indicate the positions of transition temperatures from Monte Carlo (T_{DO_3}, T_{B2}) and mean-field ($T_{DO_3}(MF)$, $T_{B2}(MF)$) approximations.

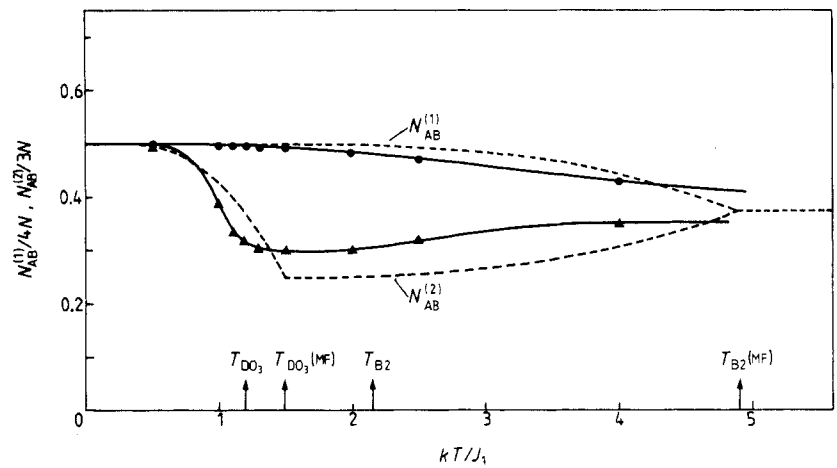

Figure 4. Normalised number of nearest- ($N_{AB}^{(1)}$) and next-nearest- ($N_{AB}^{(2)}$) neighbour AB pairs for $x = 0.75$ and $W = 0.25$ and different values of temperature T_q. ●: $N_{AB}^{(1)}$; ▲: $N_{AB}^{(2)}$ obtained from Monte Carlo simulations. The full curves are just guides to the eye. The broken curves are the mean-field solutions.

$N_{AB}^{(2)}$ displays a remarkable decrease in the DO_3 region, remains almost constant in the B2 phase, and slowly increases in the A2 region.

We have also performed Monte Carlo studies slightly below ($x = 0.70$) the stoichiometric composition. At low temperatures, complications arise from the high

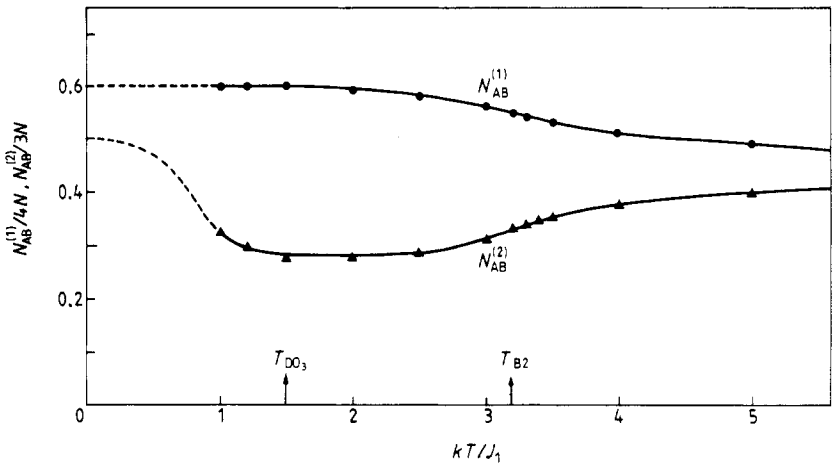

Figure 5. Normalised number of nearest- ($N_{AB}^{(1)}$: ●) and next-nearest- ($N_{AB}^{(2)}$: ▲) neighbour AB pairs for $x = 0.70$ and $W = 0.25$ obtained from Monte Carlo simulations. The full curves are guides to the eye. The broken curves are extrapolations to theoretical values at $T = 0$ K.

degeneracy of the ground state which prevents the system from reaching the proper equilibrium state in a reasonable time. The behaviour obtained for both $N_{AB}^{(1)}$ and $N_{AB}^{(2)}$ (figure 5) is similar to the one obtained in the stoichiometric case.

From these results we argue that the temperature behaviour of properties depending on $N_{AB}^{(1)}$ and $N_{AB}^{(2)}$ will be mainly distorted near the T_{DO_3} ordering transition. In particular, taking into account equation (12), after quenches from T_q to very low temperatures, this effect should be found in the elastic constants C_{11}, C_{44}, and C' as well as in the martensitic transition temperature M_s (see equation (15)). It is interesting to note that from our results we expect, in the DO_3 region, more important relative changes with ordering in C' than in C_{44}. When considering the elastic constant C_{11}, predictions cannot be done in such a straightforward way because of its simultaneous dependence on both $N_{AB}^{(1)}$ and $N_{AB}^{(2)}$. To proceed further, an analysis of the sign and relative magnitude of $\tilde{\Phi}_j^{(1)}$ and $\tilde{\Phi}_j^{(2)}$ is required. In the B2 region, C_{44} and C' exhibit relative variations with ordering of the same order of magnitude. As before, the expected behaviour for C_{11} needs a more elaborate analysis. In certain cases, the terms depending on $N_{AB}^{(1)}$ and $N_{AB}^{(2)}$ could balance each other and give rise to a very weak variation of C_{11} with ordering. This is in agreement with previous experimental results corresponding to the B2–A2 transition in Cu–Zn (MacManus 1969). Following our arguments this implies that changes of elastic anisotropy with ordering are mainly associated with changes in C'.

Very recently we have analysed the behaviour of the resolved shear stress to induce the martensitic transformation in two Cu–Zn–Al alloys as a function of quenching T_q temperatures (Planes *et al* 1989). Such an alloy can be viewed, to ordering effects, as a binary alloy. This is because ordering energies for the CuAl pairs are about 1.5 times greater than for CuZn pairs, but around 20 times greater than for ZnAl pairs (Ahlers 1986, Castán and Planes 1989). By using the Clausius–Clapeyron equation, it is possible to obtain the corresponding shift of the M_s temperature, ΔM_s, after quenches from the temperature T_q. It has been obtained that the equilibrium state at T_q can be frozen-in at low temperature by fast quenches if $T_q < 600$ K. For temperatures above this, reordering takes place to a significant degree during the quench due to a large vacancy concentration in the system.

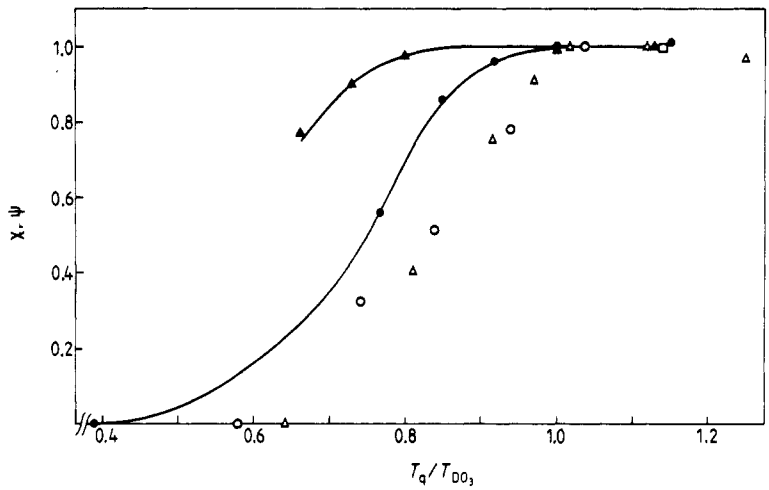

Figure 6. Representation of $\chi = (N_{AB}^{(2)}(T_q) - N_{AB}^{(2)}(0))/(N_{AB}^{(2)}(T_{DO_3}) - N_{AB}^{(2)}(0))$ as a function of the reduced temperature T_q/T_{DO_3} for the system with $x = 0.70$ (▲) and $x = 0.75$ (●). The behaviour of χ with T_q is compared with experimental values of $\psi = (M_s(T_q) - M_s^*)/(M_s(T_{DO_3}) - M_s^*)$ corresponding to two Cu–Zn–Al alloys with Cu atomic fractions of 0.619 (○) and 0.633 (△).

For the two alloys considered here, the composition is: 61.96 at.% Cu; 28.09 at.% Zn for alloy A, and 63.37 at.% Cu; 25.26 at.% Zn for alloy B. The corresponding order–disorder temperatures are: $T_{DO_3} = 460$ K and $T_{B2} = 825$ K for alloy A, and $T_{DO_3} = 500$ K and $T_{B2} = 825$ K for alloy B. Following the previous argument, the DO_3–B2 transition should then be suppressed by fast quenches from temperatures above 500 K. Consequently, the effect of the B2 ordering alone on the M_s temperature can be analysed after quenches from T_q temperatures ranging between 500 and 600 K. In figure 6 we have plotted $(N_{AB}^{(2)}(T_q) - N_{AB}^{(2)}(T_q = 0\,\text{K}))/(N_{AB}^{(2)}(T_q = T_{DO_3}) - N_{AB}^{(2)}(T_q = 0\,\text{K}))$ as a function of T_q/T_{DO_3} obtained from Monte Carlo simulations for the alloy A_xB_{1-x}, with $x = 0.70$ and 0.75. This quantity is compared with experimental values of $(M_s(T_q) - M_s^*)/(M_s(T_{DO_3}) - M_s^*)$ as a function of T_q/T_{DO_3} corresponding to the Cu–Zn–Al alloys considered. M_s^* is the MPT temperature measured after air cooling from $T_q = 1093$ K and aging at room temperature. After this temperature treatment the degree of atomic order is very close to the maximum at room temperature. Indeed, we note that the two curves show the same qualitative behaviour. Up to T_{DO_3}, M_s decreases as T_q increases and remains practically constant for T_q above this temperature. This is the expected behaviour in view of equation (15) and the behaviour of $N_{AB}^{(2)}$ with temperature (figure 5). In addition, it is interesting to note that this decrease of both M_s and $N_{AB}^{(2)}$ after quenches from T_q temperatures in the DO_3 region enables us (taking into account equation (14)) to conclude that C' increases in this region. This result means that for the class of alloy considered here, the term $\tilde{\Phi}_f^{(2)} > 0$.

4. Conclusions

We have studied the atomic order dependence of elastic constants of BCC binary alloys near the A_3B composition. The elastic constants are obtained at $T = 0$ K for frozen-in configurations quenched from different temperatures T_q across the stability regions of

the three phases DO_3, B2 and A2. At each temperature T_q, the equilibrium configuration is obtained by means of Monte Carlo simulations of an Ising model for such an alloy.

Assuming central pairwise additive forces, we deduce that the shear moduli C_{44} and C' depends linearly on the number of NN ($N_{AB}^{(1)}$) and NNN ($N_{AB}^{(2)}$) AB pairs respectively, whereas C_{11} depends on both $N_{AB}^{(1)}$ and $N_{AB}^{(2)}$. Given that in the DO_3 region $N_{AB}^{(2)}$ exhibits a more remarkable variation with temperature than $N_{AB}^{(1)}$, we expect that C' will depend more strongly on the state of order than C_{44}. In the B2 and A2 regions $N_{AB}^{(1)}$ and $N_{AB}^{(2)}$ present comparable variations with temperature. Consequently, C' and C_{44} should exhibit relative variations with order of similar magnitude.

The results show important relative changes of the elastic constant C' with ordering after quenches from $T_q < T_{DO_3}$, and a nearly constant value when $T_q > T_{DO_3}$. This behaviour is found to be in qualitative agreement with experimental data on the M_s temperature of Cu–Zn–Al alloys, measured after quenches from temperatures T_q, and it is independent of the fine detail of the interatomic potential.

References

Ahlers M 1986 *Prog. Mater. Sci.* **30**
Bell J M 1987 *Physica* A **142** 22–37
Binder K 1984 *Applications of Monte Carlo Methods in Statistical Physics* (Berlin: Springer)
Born M and Huang K 1956 *Dynamical Theory of Crystal Lattices* (Oxford: Clarendon)
Castán T and Planes A 1988 *Phys. Rev.* B **38** 7959–65
—— 1989 *J. Mater. Sci.* **24** 974–8
Castán T, Planes A, Ramos A and Viñals J 1989 *Phys. Rev.* B **39** 3551–3
Delaey L, Krishnan R V, Tas H and Warlimont H 1974 *J. Mater. Sci.* **9** 1521–35
Dünweg B and Binder K 1987 *Phys. Rev.* B **36** 6935–52
Gooding R J and Krumhansl J A 1988 *Phys. Rev.* B **38** 1695–1704
—— 1989 *Phys. Rev.* B **39** 1535–40
Guénin G and Gobin P F 1982 *Metall. Trans.* A **13** 1127–34
Guénin G, Morin M, Gobin P F, Dejonghe W and Delaey L 1977 *Scr. Metall.* **11** 1071–5
Gunton J D and Droz M 1983 *Introduction to the Theory of Metastable and Unstable States* (Berlin: Springer)
Lindgård P-A and Mouritsen O G 1986 *Phys. Rev. Lett.* **57** 2458–61
MacManus G M 1969 *Phys. Rev.* **129** 2004–7
Massalski T B and King H W 1961 *Prog. Mater. Sci.* **10** 1–78
Milstein F 1970 *Phys. Rev.* B **2** 512–18
Nakanishi N, Murakami Y and Kachi S 1968 *Scr. Metal.* **2** 673–6
Planes A, Guénin G and Macqueron J L 1985 *J. Phys. F: Met. Phys.* **15** 1203–11
Planes A, Macqueron J L, Morin M and Guénin G 1981 *Mater. Sci. Eng.* **50** 53–7
Planes A, Romero R and Ahlers M 1989 *Acta Metall.* at press
Rapacioli R and Ahlers M 1979 *Acta Metall.* **27** 777–84
Ray J R 1988 *Comput. Phys. Rep.* **58** 109–52
Richards M J and Cahn J W 1971 *Acta Metall.* **19** 1263–77
Romero R and Ahlers M 1989 *J. Phys: Condens. Matter* **1** 3191–200
Roy D, Manna A and sen Gupta S P 1974 *J. Phys. F: Met. Phys.* **4** 2145–51
Squire D R, Holt A C and Hoover W G 1969 *Physica* A **42** 388–97
Viñals J, Torra V, Planes A and Macqueron J L 1984 *Phil. Mag.* A **50** 653–66
Ye Y-Y, Chen Y, Ho K-M, Harmon B N and Lindgård P-A 1987 *Phys. Rev. Lett.* **58** 1769–72
Zener C 1947 *Phys. Rev.* **71** 846–51